EPJ E
Soft Matter and Biological Physics
EPJ.org
your physics journal

Eur. Phys. J. E (2016) **39**: 94 DOI 10.1140/epje/i2016-16094-5

Water populations in restricted environments of lipid membrane interphases

Laureano M. Alarcón, M. de los Angeles Frías, Marcela A. Morini, M. Belén Sierra, Gustavo A. Appignanesi and E. Anibal Disalvo

edp sciences Società Italiana di Fisica Springer

Eur. Phys. J. E (2016) **39**: 94
DOI 10.1140/epje/i2016-16094-5

THE EUROPEAN PHYSICAL JOURNAL E

Regular Article

Water populations in restricted environments of lipid membrane interphases

Laureano M. Alarcón[2,a], M. de los Angeles Frías[1], Marcela A. Morini[2], M. Belén Sierra[2], Gustavo A. Appignanesi[2,b], and E. Anibal Disalvo[1,c]

[1] Laboratorio de Biointerfases y Sistemas Biomiméticos, Laboratorios Centrales, CITSE-UNSE, Santiago del Estero, Argentina
[2] Sección Fisicoquímica, INQUISUR-UNS-CONICET, Universidad Nacional del Sur, Av. Alem 1253, 8000-Bahía Blanca, Argentina

Received 27 May 2016 and Received in final form 14 August 2016
Published online: 21 October 2016 –

Abstract. We employ molecular dynamics simulations to study the hydration properties of Dipalmitoylphosphatidylcholine (DPPC) bilayers, both in the gel and the liquid crystalline states. We show that while the tight hydration centers (PO and CO moieties) are significantly hydrated in both phases, the gel-fluid transition involves significant changes at the second hydration shell, particularly at the buried region between the hydrocarbon tails. Thus, while almost no buried water population exists in the gel state below the carbonyls, this hydrophobic region becomes partially water accesible in the liquid crystalline state. We shall also show that such water molecules present a lower H-bond coordination as compared to the molecules at the primary hydration shell. This means that, while the latter are arranged in relatively compact nanoclusters (as already proposed), the buried water molecules tend to organize themselves in less compact structures, typically strings or branched strings, with a scarce population of isolated molecules. This behavior is similar to that observed in other hydration contexts, like water penetrating carbon nanotubes or model hydrophobic channels or pores, and reflects the reluctance of water to sacrifice HB coordination.

Introduction

Water is the essential solvent that stabilizes the structure of cell membranes and proteins. Although several evidences are available confirming that water is a component of membrane structure, its possible functional role has not been considered in detail on thermodynamic and modelistic grounds [1]. Most of the processes in biological membranes have been analyzed under the paradigm that the lipid bilayer, formed by a hydrocarbon core hidden from water and polar head groups facing the aqueous phase, is a static, low dielectric slab impermeable to ions and polar solutes [2,3]. On the other hand, membranes have been proposed as responsive structures in the sense that they may "react" to the presence of different compounds in the aqueous media adjacent to the membrane (effectors) [4]. However, in this picture water is not considered as a necessary component of the membrane involved in its response to physical chemical changes in the surrounding media. Instead, the proposal that water may be the key to modulate global and specific interactions between biomolecular surfaces can be justified on biological and physicochemical grounds. The biological reason is given by the fact that water should be present in living systems in a liquid state. Although cells and tissues can be preserved dry in the presence of compounds that mimic water, restoration of liquid water is essential for cell growing, metabolism and signal response [2,5,6]. From the physicochemical view point, such requirement stems from the fact that water is the only compound that is able to buffer free energy changes due to its high surface tension. Taken together, both reasons imply that water is a dynamic constituent in membranes that may act as anthenna for biological signals to control activities of membrane-bound enzymes and to trigger cell recovery and survival in stress processes [7]. This hypothesis is based on the fact that the thermodynamic activity of water at the lipid-water interface determines the surface pressure (surface tension) of the lipid interface. Modulation of surface pressure via water activity may affect the interaction of aminoacid motifs found in peptides and proteins acting as signals or effectors on cell membranes and the activation or inactivation of interfacial enzymes [8,9].

In pure water, molecules in the surface lose the tetrahedral coordination they have in bulk water, giving place to a high surface tension as a result of non-compensated

[a] e-mail: lalarcon@uns.edu.ar
[b] e-mail: appignan@criba.edu.ar
[c] e-mail: disalvoanibal@yahoo.com.ar

hydrogen bonds. This uncompensation creates an excess of surface free energy that decreases when lipid molecules are added to the surface to form a monolayer. At a surface pressure of 42–45 mN/m phospholipid monolayers collapse and this excess disappears turning the interphase unresponsive to effectors added to the subphase. The critical surface tension in monolayers (cut off pressure) at which no response in terms of surface pressure changes are observed when enzymes, proteins or lytic components are added underneath the monolayer has been related to the excluded volume of water around the head group that has no solvent properties. This excluded volume of the lipids is ascribed to the *primary hydration shell* of the head groups which can be displaced only by H-bond compounds that mimic water structure, such as sugars and polyols after drastic procedures of dehydration [10,11]. In contrast, changes in surface pressure are observed by the addition of aminoacids, peptides or proteins to the subphase if monolayers are at lower surface pressures with respect to that of collapse. The lowering of surface pressure at which the response is produced implies the presence of an excess of water beyond that primary hydration shell of the phospholipids. This water population identified as *second shell* is water confined beyond the hydration shell of the phospholipid head groups [7,11,12]. The relevance of water organization at this level is not known and possibly it may be a link between stressed states governed by lateral pressure in the membrane as a mechanochemical device and by osmosis [13]. The response in surface pressures below the critical one is expected to be related to the particular organization of the water molecules hydrating the membrane [8,14]. To feature these states, the membrane should be defined as a thermodynamic system. This is to say that the hydration levels should be considered in the generation of regions with an excess of surface free energy that would be responsible for triggering the response to biological effectors [4,15]. The thermodynamic state of this second shell hydration water can be characterized by the water activity determined by the activity coefficient which depends on the structural organization of the hydrogen bonds the water molecules establish between themselves and with the lipid groups. Such water arrangements in restricted environments (defined in time and space, and according to their H-bond coordination) would conform informational units that may be involved in membrane response. Due to the great variation in lipid composition giving place to versatility, one would expect a number of water configurations giving place to versatility, cooperativity and synergisms [10]. A similar proposal has been made for proteins [16,17] and water clusters necessary for preserving living structure has been proposed as dessicons [18].

In a previous paper, it was observed by Fourier Transform Infrared spectroscopy that the bands corresponding to bulk water were modified in the presence of membranes in the gel state and membranes in the liquid crystalline state [19]. The deconvolution of the water bands denoted, at least, five populations of water species. At a first approximation it is possible to assign each band to waters forming 0, 1, 2, 3, 4 hydrogen bonds. However, each band is broad enough to interpret that several configurations of water with the same number of H bonds contribute to them. These water populations can be the average of those formed between water themselves and with the membrane groups [19]. This would account for multiple arrangements of H bonds around a mean value of energy. Whether these configurations are H bonds between water molecules themselves facing hydrocarbon regions or with residues such as CO or PO is a matter of study. In this regard, the water bands were correlated with a redistribution of hydrated and non-hydrated carbonyl groups [20]. This indicates that changes in the hydration of the lipid moieties are concomitant with changes of the water arrangements at the adjacence of the membrane. However, how many water molecules are involved in each configuration is ignored.

On the basis of the above expounded scenario, it becomes essential to gain a detailed insight on water organization at the lipid/water interphase by classifying water molecules in each residue of the lipids (both at the hydrophilic and hydrophobic regions) and clasifying the hydrogen-bond coordination of such water molecules so as to determine the way in which membrane water accumulates excess free energy to drive the interaction of effectors with the membrane.

Methologies

Simulation details

Dipalmitoylphosphatidylcholine (DPPC) bilayers were simulated by means of AMBER12 package [21]. The bilayer was composed of 128 DPPC molecules (64 per monolayer in a 8×8 arrangement). The initial separation between DPPC was 9 Å in a triangular arrangement. The membrane was stabilized at 323 K for the liquid crystalline state and at $T = 298$ K for the gel state and solvated with a total of 10443 TIP3P water molecules (which means around 81 water molecules per lipid) in order to assure that the system was fully hydrated. Solvation was done along the Z axis and the system was subjected to periodic boundary conditions along the (X, Y) plane. All the atoms of the bilayer were fixed during minimization and temperature and pressure stabilization. The minimization was carried out in two steps, both at constant volume. In the first step we minimize the solvent, keeping fixed the membrane, and then release it and minimize the entire system. After stabilizing the system temperature using the Langevin thermostat and keeping fixed the bilayer, we proceeded to equilibrate the dimensions and density of the system. Then, all restraints were removed and the bilayer was free to establish a lipid-lipid equilibrium distance. After 50 ns equilibration, an area per lipid of around 62 Å is obtained for the bilayers at $T = 323$ K, a result consistent with experimental values [22]. Both equilibration and final production data used a NPT assembly, with the SHAKE activated for bonds with hydrogens.

Calculation of the number of water molecules per lipid was obtained after equilibration of the bilayers. This was

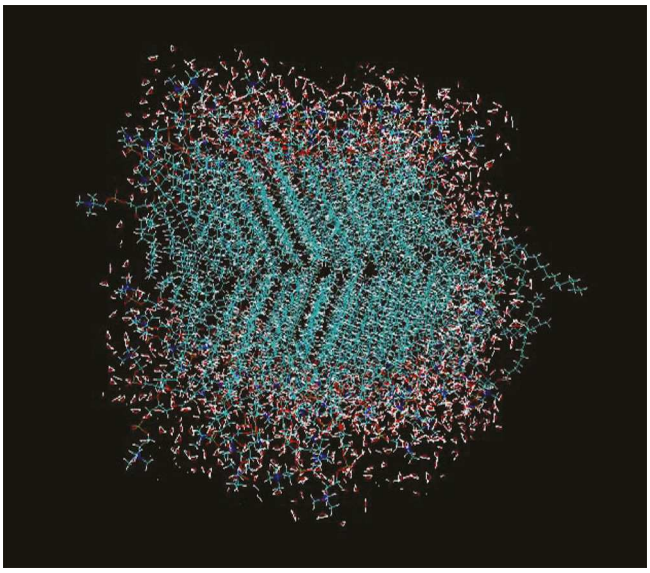

Fig. 1. Snapshop of one of the simulation runs displaying the lipid bilayer and the water molecules that are proximal (first neighbors) to the lipid chains. For the sake of clarity, we omit the rest of the water molecules of the simualtion box.

performed by counting all the water molecules whose distance to the lipid is lower than certain threshold value (chosing a cut off of 4.5 Å). This procedure includes molecules hydrating the exposed polar heads and also water molecules that have penetrated the bilayer. The number of water molecules per lipid in the liquid crystalline state at this temperature is 23.2 (while it amounts to 18.3 if we use a threshold of 4.0 Å instead). This value is consistent with experimental findings [23]. To further classify water molecules we define water content around lipid groups in a way such that each water molecule is exclusively assigned to its first lipid neighbor group (thus, a water molecule that might be considered neighbor to more than one different lipid group according to a distance criterion, is here exclusively assigned to its closest lipid group so as to be counted only once). For example, each CH of the choline roughly has 6 water molecules in a sphere of 4.5 Å in the liquid crystalline phase, but only 2 are first neighbors while the others are first neighbors of other groups. Figure 1 shows a snapshop of a simulation run displaying both the lipids and their first neighbor water molecules. All other water moleucles of the simulation box are omitted for clarity.

Quantifying local hydrophobicity

A simple very appealing measure of local hydrophobicity is provided by the quantification of water density fluctuations [24,25]. Water density fluctuations at differently functionalized self-assembled monolayers (SAMs) have been characterized demonstrating that hydrophobic-like surfaces present much larger density fluctuations than the ones displayed by hydrophilic-like surfaces, thus providing a good quantitative measure of hydrophobicity [24,25]. Normalized fluctuations of water number density, $\sigma^2/\langle N\rangle^2$ in small observation volumes (where N is the number of water molecules within such volume) are approximately equal to $2\mu^{\mathrm{ex}}/kT$, where μ^{ex} is the free energy of formation of cavity of such radius [24,25]. Thus, a high value of the normalized density fluctuations at a given place indicates a favorable work of cavity creation at such place and, thus, a high hydrophobicity. In this work, water density fluctuations at the head groups of the phospholipid membranes in comparison, density fluctuation on self-assembled (alkane-like) monolayers (SAMs) functionalized in order to be hydrophobic or hydrophilic (chain heads with CH_3 or OH groups respectively) are evaluated. At variance from the previous settings where the alkyl chains were rigid [24–27], in the present studies the chains will be flexible and, thus, water density fluctuations within observation spheres centered at the heavy atoms of the groups of interest which thus move with the atom are calculated. The probability distributions for observing N water molecules, $p(N)$, within a small spherical observation volume of radius 4.0 Å centered at the C of the methyl heads of the hydrophobic SAMs, at the O of the alcohol head groups of the hydrophilic SAMs [24–27] and at different heavy atoms of the head groups of the phospholipid membranes are calculated. A high probability of having zero water molecules in the observation domain, and thus a high value of density fluctuations, implies an enhanced propensity for dehydration or high hydrophobicity.

Results

In fig. 2, water populations around membrane groups in the gel (black bars) and in the liquid crystalline (grey bars) state are compared. Direct inspection shows that all the lipid groups increase their hydration in the liquid crystalline state as compared to the gel state. The overall number of water molecules per lipid is 23.2 for the liquid crystalline state while it amounts to only 10.0 molecules for the gel state. It is thus evident that there is a relative difference in water content between the two phases at the head group region with different magnitudes at the cholines, the phosphate and carbonyl oxygens. However, the most important changes are found at the regions close to the carbonyl groups (but not at the carbonyl themselves), identified as the second hydration shell and the buried water region. The relative difference in water population between gel and liquid crystalline states at these non-polar regions is very significant. Namely, the water content at the O and C atoms from O4 to O6 and from C3 to C5 is drastically reduced in the gel state as compared with the liquid crystalline state. More notably, this figure shows that virtually no water population is found for all the carbon atoms from C6 to C16 in the gel state, while a non-negligible water content is exhibited by these atoms in the liquid crystalline state. This means that while almost no buried water population exists in the gel state, the hydrocarbon chains become partially water accesible in the liquid crystalline state. However, the water content

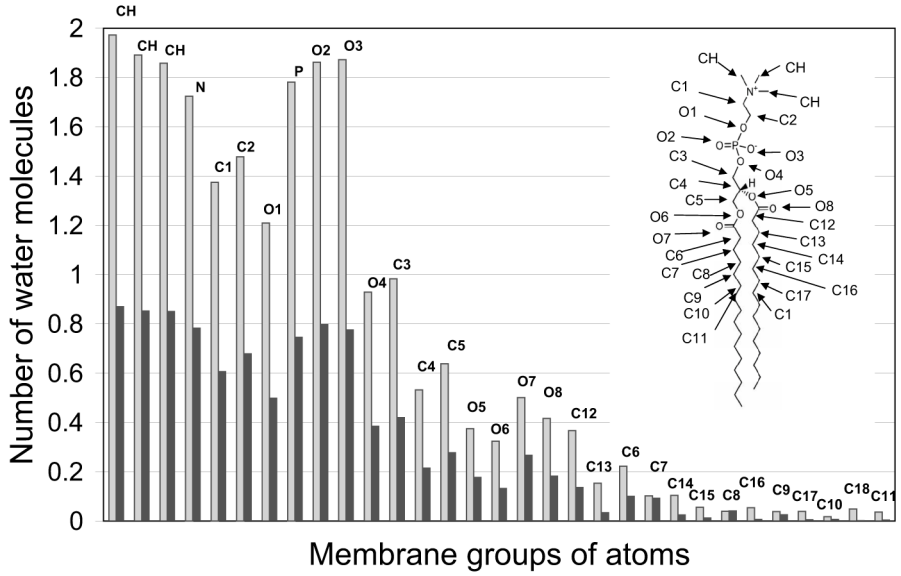

Fig. 2. Populations of water molecules around lipids in the gel (dark gray bars) and in the liquid crystalline state (light gray bars).

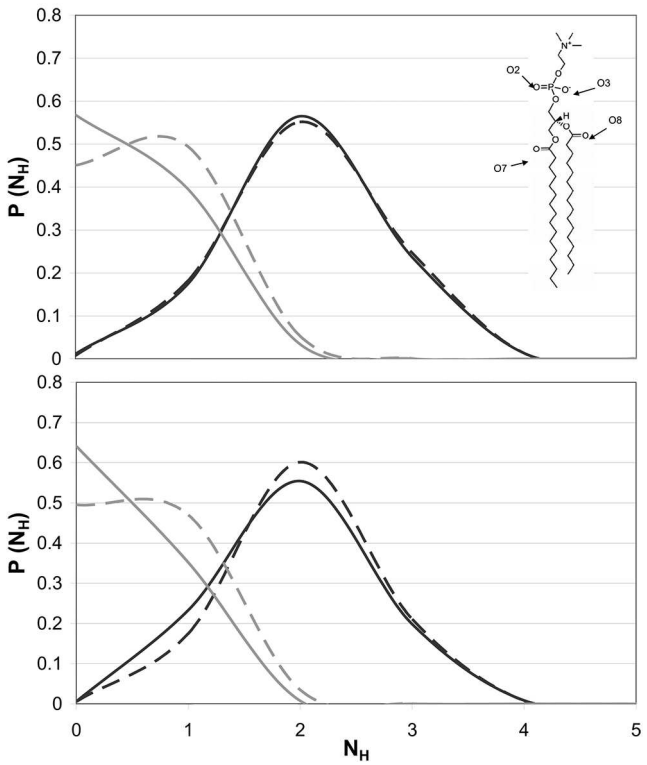

Fig. 3. Distribution of H bonds around the different head groups ($P(N_H)$) in the liquid crystalline (top) and gel (bottom) phases: Dark continuous line for O3, dark dotted line for O2, gray continuos line for O8 and gray dotted line for O7 groups of atoms.

is low, thus indicating only partial hydration and transient water molecules.

In fig. 3 the distribution of hydrogen bonds of water molecules in the different lipid groups in both the liquid crystalline and gel states is analyzed. It is observed that two H bonds are found for the oxygens of the phosphate (from the roughly 6 water molecules that are found around each phosphate within a distance of 4.5 Å). Thus, both oxygens of the phosphate group of the lipid chain saturate their H-bond capability and possess two kinds of water molecules: directly bound by H bonds and non-bonded molecules. In turn, the carbonyl group of the sn_2 chain forms only one H bond with water molecules, while the CO of the sn_1 chain is mostly not hydrogen bonded and thus, is not significantly hydrated. This is consistent with experimental findings [20]. The similarity of the curves in both the liquid crystalline and gel states speaks of the fact that the H-bonded water molecules are not lost upon the liquid to gel transition.

In fig. 4a we show how the different water species (according to the types of H bonds they form) are distributed in the groups of the membrane both above and below the transition temperature. The sequence WPC indicates the number of H-bonds the water molecule forms with other water molecules, PO and CO, respectively. For instance, 100 denotes one H-bond with water and none with PO and CO; 210 indicates two H-bonds with water, one with PO and none with CO; 301 means three H-bonds with water, none with PO and one with CO, and so on. It is observed that most of the water molecules form three H bonds with other water molecules (300 species). A lower number of water molecules form 2 or 4 water-water H bonds. Finally, a much lower amount of water molecules bound to phosphates (110, 210 and 310 species) is found. If we classify water molecules by the total number of hydrogen bonds they form (regardless these H bonds are water-water or water-lipid H bonds), the lipid hydration water would present a distribution very similar to that of bulk water (data not shown). This distribution would be dominated by the water molecules at the polar head groups, since the population below the CO moieties is low. In turn,

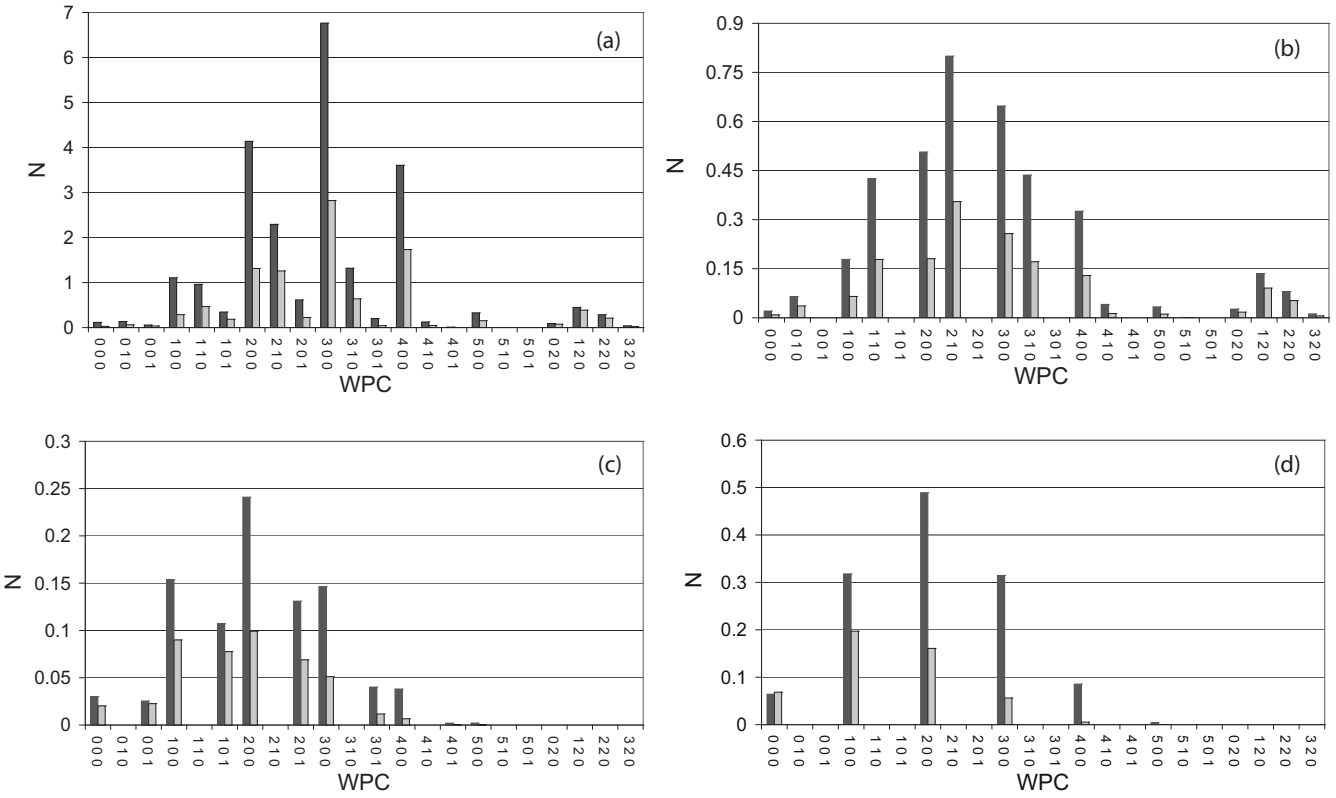

Fig. 4. Different water species distributed around the different groups of the membrane, indicated according their H-bond partners. The sequence is called WPC, where the three digits indicate the number of H-bonds it forms with other water molecules, PO and CO, respectively. For instance, 100 denotes one H-bond with water and none with PO and CO, 210 indicates two H-bonds with water, one with PO and none with CO, 301 means three H-bonds with water, none with PO and one with CO, and so on. Black bars: Liquid crystalline state; light gray bars: Gel state. a) For the whole hydration water. b) For the water molecules hydrating the phosphates. c) Water around the carbonyls. d) Buried water (beyond the carbonyles). e) Examples of configurations of water nanoclusters and strings around the lipid chains.

figs. 4b and 4c and 4d discriminate the behavior for the regions around the tightly hydration centers (phosphates and carbonyls) and for the buried region (the carbon tails below the CO), respectively. Figures 4b and 4c are consistent with previous simulation results [28,29]. It is interesting to note that water molecules buried between the hydrocarbon chains below the carbonyls present a lower H-bond coordination. However, the negligible population of 000 (that is, uncoordinated molecules) implies that water molecules are arranged in (low H-bond coordination) clusters at such region but do not penetrate in isolation. At the tight hydration centers (CO and PO) the H-bond coordination is higher, a fact consistent with the recent finding of water nanoclusters at such regions [30]. Thus, our results confirm the existence of such relatively compact water nanoclusters at the tight hydration centers. However, we also find here the existence of less compact (strings or ramified strings) nanoclusters at the buried region within the hydrocarbon chains. Figure 4e depicts some instances of such kind of objects. While no simple topological description of such kind of "objects" is possible given the disordered environments of the lipid chains, we do find a different behevior at the polar lipid moieties and at the hydrophobic tails. It is clear form fig. 3b that around the phosphates the two most prevalent hydrogen bond configurations are given by water molecules with three hydrogen bonds (HB): three water-water HBs (WPC = 300) and two water-water and 1 water-phosphate HBs (WPC = 210). This is compatible with relatively compact arrangements as in the regions around the phosphates depicted in fig. 4e. However, below the carbonyls (fig. 4d; the buried water or water molecules deeper inside the bilayer facing the hydrocarbon chains) the configuration that predominates is WPC = 200: water molecules hydrogen bonded to other two water molecules. This is consistent with a string-like organization (branched are also found in certain cases and imply the existence of a WPC = 300 molecule, which has lower but non-negligible probability). These kinds of strings are evident in fig. 4e for water molecules that have penetrated below the carbonyls (short chains of 2, 3 or 4 water molecules in the examples shown).

In fig. 5, local hydrophobicity is quantified by means of water density fluctuations [24–27] at the head groups of the phospholipid membranes. For comparison, density fluctuations on self-assembled functionalized hydrophobic or hydrophilic alkane-like monolayers (SAMs) were also calculated. Specifically, the probability distributions for

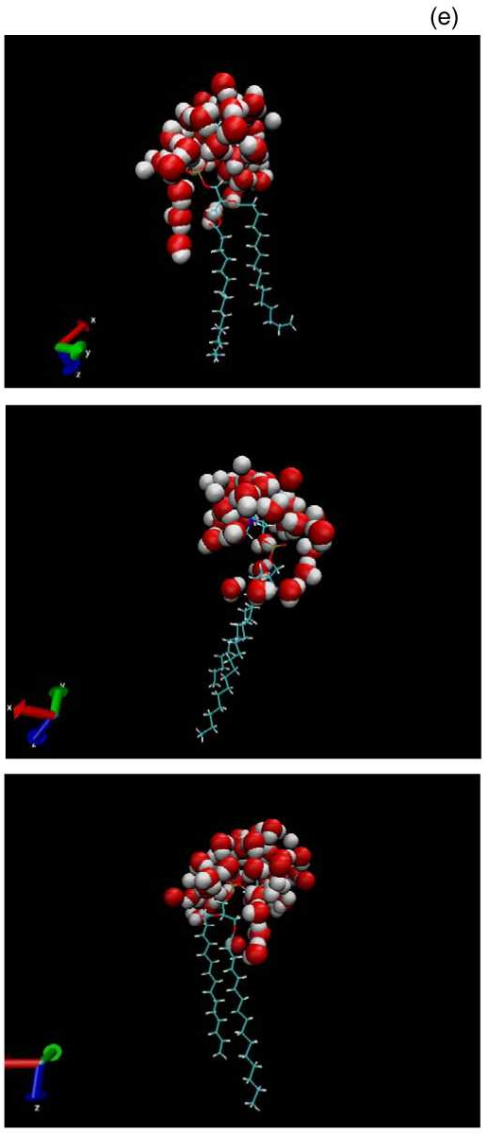

Fig. 4. (Continued.)

observing N water molecules, $p(N)$, within a small spherical observation volume of radius 4.0 Å centered at different heavy atoms of the head groups of the phospholipid membranes is displayed in such figure. Different probabilities for exhibiting zero water molecules in the spherical domain are observed for the different groups. Phosphate oxygens (O2 and O3) are the most hydrophilic moieties of the lipid bilayer with a hydrophilicity similar (or even higher) to the hydrophilic SAM. The C4 carbons are the most hydrophobic groups presenting density fluctuations similar to the ones of the hydrophobic SAM while the rest of the groups display an intermediate behavior. As evident from such figure, the different oxygens present different hydrophilic degrees, as also happens for the comparative hydrophobic behavior of different carbonaceous groups. A first lesson emerging from this figure is, thus, that the hydrophobicity of a given group can vary significantly depending on its local environment, where both the local chemistry and geometry can play a role. The gel state presents slightly more hydrophobic environments, particularly at regions deeper inside the membrane.

Discussion

A *résumé* of the water increase and H bond populations at each membrane groups is given in table 1. The total number of water molecules per lipid in the liquid crystalline state is nearly two-fold larger than in the gel state. The number of water molecules directly bound to the different groups can be inferred from the calculation of H bonds, a value that amounts to 5 water molecules. Thus, comparing the total number of water molecules in the liquid crystalline state with those directly bound, it turns out that there are 17 water molecules unbound to the lipid in the second shell.

Table 1. Distribution of water molecules and H bonds in membrane chemical groups of phosphatidylcholine bilayers in the liquid crystalline state: I) O in the phosphate group; II) O carbonyl group (sn_1 acyl chain); III) O carbonyl group (sn_2 acyl chain); IV) Methylenes of the choline; V) N-choline; VI) Methylenes of the ethanolamine; VII) Glycerol moiety; VIII) Total.

		I	II	III	IV	V	VI	VII	VIII
Gel	Water molecules	2.8	0.3	0.2	2.6	0.8	1.3	1.7	9.7
Liquid crystalline	Water molecules	6.3	0.6	0.5	5.6	1.7	2.8	3.8	21.3
	Number of H bonds	4	1	–	–	–	–	0	5
	Water molecules 1st *hydration shell*	4	1	–	–	–	–	0	5
	Water Molecules 2nd *hydration shell*	2	1	0.5	6	1.7	3.8	2.3	17.3

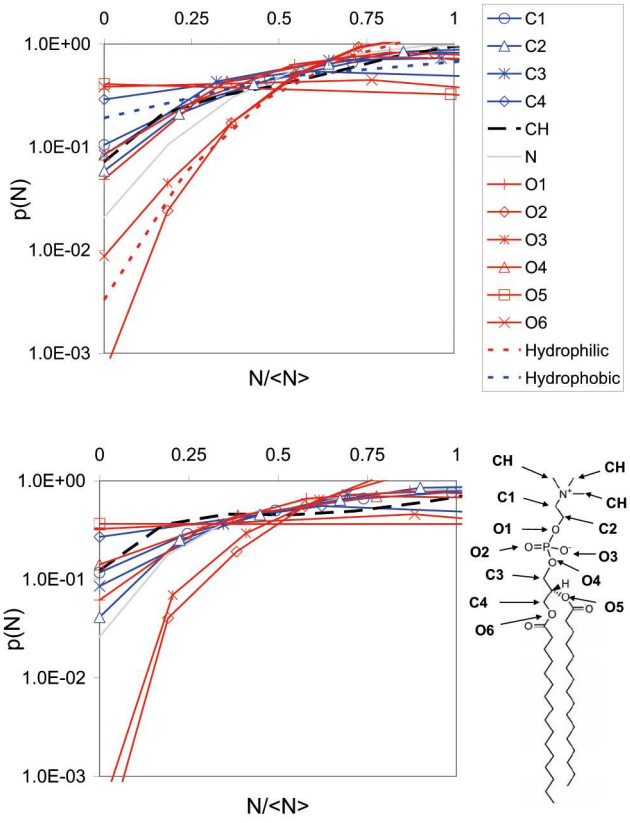

Fig. 5. Hydrophobicity-hydrophilicity ratio for the lipid membrane in the liquid crystalline state.

Congruent with the change in water bands observed by FTIR when lipids go from the gel to the liquid crystalline state [19], groups or regions that increase in one or two water molecules from the gel to the liquid crystalline state are PO, CO, C_1 and C_2 at the polar group. Thus, the area per lipid increase reported by Nagle [22] and Disalvo [1] at the phase transition is due to the incorporation of one-two water molecules per group. This change in area involves a tiny increase in terms of number of water molecules but, in contrast, is extremely significant in terms of surface free energy since its incorporation turns the membrane into a responsive structure.

The phase transition affects the hydration centers such as PO and CO and also the region below the phosphate groups and corresponds to water molecules in contact with carbonyl groups and the hydrocarbon chains. This region could be defined as the second hydration shell beyond the first hydration shell of the phosphate (which is very tightly bound) and it may be affected by the carbonyl groups oriented at the water/hydrocarbon interface as reported by FTIR [19,31]. Buried water would involve water affected by the hydrocarbon chains below the carbonyl groups (or deeper inside) [32].

The important conclusion with this result is that, besides the increase in hydration number at the polar moieties, the most notable change is due to water entering in restricted spaces facing non-polar groups below the phosphates and beyond the carbonyl groups (as clearly illustrated by fig. 2). This is completely in accordance with the increase in area per lipid and the total number of water per lipid observed experimentally [1,22]. In other words, fig. 2 shows that the most significant *relative* differences betweent the liquid crystalline and gel states involve water molecules at the second shell, while primary hydration waters remain roughly unchanged (CO and PO moieties remain significantly H-bonded in both states). This change in water species is concomitant with the surface pressure increase observed at constant area in the surface pressure/area per molecule isotherms, probably involving intermediate and buried waters affected by the thermal or mechanical expansion. Thus, the expansion of the interchain region that accompanies the phase transition allows for water penetration at the intermediate region, located between the PO and CO moieties, and at the buried region, confined below the carbonyl chains.

The present study demostrates that at the phase transition water molecules below the phosphates and near the carbonyl groups correlate with the changes in the hydrated/non-hydrated populations of carbonyl groups at the water hydrocarbon interface found by FTIR [19, 33]. They would correspond to different water species in its adjacencies suggesting a correspondence between wall quality and water arrangements. It is concluded by the hydrophilic-hydrophobic balance shown in fig. 5 that the density fluctuations in this region implies an enhanced

propensity for dehydration, a favorable work of cavity creation at such place and, as a consequence, a high hydrophobicity [24,25]. Such high hydrophobicity regions would be related to the organization of a few undercoordinates water molecules (*i.e.* with a low number of H bonds) determining a local excess in surface free energy and, as well, a local affinity of the membrane for effectors like aminoacid and peptide residues. Thus, the state of the lipid membrane as a responsive structure would be related to the presence of those water subpopulations with low H bond coordination (excess free-energy water molecules). The presence of non-compact clusters of water molecules in the form of strings or branched strings at such region is consistent with this scenario.

On quantitative grounds, fig. 2 denotes that from C12 to C18 and from C6 to C11, *i.e.* in all the extension of the hydrocarbon chain, water is present in the liquid crystalline state while almost no water is found in the gel state. This water is statistically distributed with an average of less than one water molecule per CH_2. It reflects the fact that water is transient according to the fluctuations in the chain conformations, which is in complete agreement with FTIR results in which the CH_2 groups are connected between each other by interacting with short range forces in the gel state and that above the transition temperature the groups are isolated from each other by water molecules [14,34]. Thus, energetics expressed in terms of surface pressure is governed by the arrangements of water subpopulations that in average may concert fewer H bonds with other water molecules or with the lipid groups. Fluctuations around these combinations would allow a modulation of the orientation of the carbonyl groups in the lipid water interface and the exposure of the hydrophobic region. For this reason, surface energetics have entropic contributions due to formation/destruction of water clusters and enthalpic contributions of H bonds interactions. These effects have been described as classical and nonclassical hydrophobic interactions, respectively [35,36].

An interesting point emerges from the inspection of fig. 4d. On one side, we can see that the spectrum of water subpopulations in the buried region (below the carbonyls) is displaced to the left as compared to the one for the full membrane or for the tight hydration centers (PO and CO moieties). This fact means that water molecules at the buried hydrophobic region present a lower H-bond coordination and, thus, would represent species with an excess free energy. The water subpopulation that dominates in the liquid crystalline state at such region (we focus here our attention on the liquid crystalline state, since the gel state presents an extremely low water population at such region) is 200, with lower values for 300, 100 and a very low presence of 400 and 000 molecules. Thus, this region is dominated by the presence of less compact objects (nanoclusters), consisting mainly of string-like objects (200 coordination) or branched strings, with no significant population of isolated molecules. At any given time, a low fraction of lipids would present these string-like arrangements below the more compact nanoclusters of the polar head groups (which explains the fact that the water content at such regions is low), while the length of such objects is variable. Additionally, and at variance from the situation for the more compact nanoclusters that are always formed around all the polar head groups, these strings develop occasionally at certain positions of the bilayer. We note that a similar filling tendency has been found for carbon nanotubes [37] and for pores and tunnels carved in hydrophobic self-assembled monolayers [26,38], as we have recently shown. In such contexts, it has been shown that, due to its reluctance to sacrifice H-bond coordination, water penetrates in hydrogen-bond coordination (in certain contexts in a string-like fashion) and not in isolation [26,37,38]. Additionally, the breakdown of certain H-bonds by thermal fluctuations has been regarded as a drying inducing event in narrow pores or tunnels which show alternation of filled and empty states [26,38].

As the interaction of water molecules between themselves and with the hydrophilic or hydrophobic walls involves H bonds of different energies according to the water orientation and coordination, each structural change implies a concrete number of connected and unconnected waters, that in turn determine the hydrophilic-hydrophobic balance in the surface. In conclusion, these confined water molecules would be accountable for the responsive properties of lipid membranes.

EAD, GAA, LMA, MAF, MAM, MBS are members of the Research Career of CONICET, RA. This work was supported with funds from ANPCyT PICT 2011-2606; PICT 2012 2602, PIP CONICET 0484, PICTO 2012-0005, CiCyT (UNSE) 23A/164, PIP-CONICET-2012-2014/00193, CONICET-NSF-2012, PGI-UNS-24/Q062 and PICT-2010-1291.

References

1. E.A. Disalvo, F. Lairion, F. Martini, E. Tymczyszyn, M. Frias, H. Almaleck, G.J. Gordillo, Biochim. Biophys. Acta **1778**, 2655 (2008).
2. L.A. Bagatolli, J.H. Ipsen, A.C. Simonsen, O.G. Mouritsen, Progress Lipid Res. **49**, 378 (2010).
3. J.N. Israelachvili, Biochim. Biophys. Acta **469**, 221 (1977).
4. E. Sparr, H. Wennerstrom, Biophys. J. **81**, 1014 (2001).
5. J.H. Crowe, F.A. Hoekstra, L.M. Crowe, Annu. Rev. Physiol. **54**, 579 (1992).
6. J.H. Crowe, L.M. Crowe, Nat. Biotechnol. **18**, 145 (2000).
7. R. Costard, I.A. Heisler, T. Elsaesser, J. Phys. Chem. Lett. **5**, 506 (2014).
8. S. Damodaran, Colloids Surf. B: Biointerfaces **11**, 231 (1998).
9. E.A. Disalvo, A. Hollmann, L. Semorile, F. Martini, Biochim. Biophys. Acta **1828**, 1834 (2013).
10. V.V. Volkov, D.J. Palmer, R. Righini, Phys. Rev. Lett. **99**, 078302 (2007).
11. F. Foglia, M.J. Lawrence, C.D. Lorenz, S.E. McLain, J. Chem. Phys. **133**, 145103 (2010).
12. F.M. Goni, J.L. Arrondo, Faraday Discuss. Chem. Soc. **81**, 117 (1986).
13. T. Soderlund, J.M. Alakoskela, A.L. Pakkanen, P.K. Kinnunen, Biophys. J. **85**, 2333 (2003).
14. E.A. Disalvo, A.M. Bouchet, M.A. Frias, Biochim. Biophys. Acta **1828**, 1683 (2013).

15. K.H. Sheikh, S.P. Jarvis, J. Am. Chem. Soc. **133**, 18296 (2011).
16. R. Tsenkova, J. Near Infrared Spectrosc. **17**, 303 (2010).
17. R. Tsenkova, Spectrosc. Europe **22**, 6 (2010).
18. J.H. Crowe, Sub-cell. Biochem. **71**, 263 (2015).
19. E.A. Disalvo, M.A. Frias, Langmuir **29**, 6969 (2013).
20. M.A. Frias, E.A. Disalvo, Langmuir **25**, 8187 (2009).
21. D. Case, T. Darden, T. Cheatham III, C. Simmerling, J. Wang, R. Duke, R. Luo, R. Walker, W. Zhang, K. Merz, AMBER 12, University of California, San Francisco, CA (2012).
22. J.F. Nagle, S. Tristram-Nagle, Biochim. Biophys. Acta **1469**, 159 (2000).
23. G. Cevc, Biochemistry **26**, 6305 (1987).
24. S. Vaitheeswaran, H. Yin, J.C. Rasaiah, G. Hummer, Proc. Natl. Acad. Sci. U.S.A. **101**, 17002 (2004).
25. J.C. Rasaiah, S. Garde, G. Hummer, Annu. Rev. Phys. Chem. **59**, 713 (2008).
26. L.M. Alarcón, J.M. Montes de Oca, S.A. Accordino, J.A. Rodriguez Fris, G.A. Appignanesi, Fluid Phase Equilib. **362**, 81 (2014).
27. S.R. Accordino, J.M. Montes de Oca, J.A. Rodriguez Fris, G.A. Appignanesi, J. Chem. Phys. **143**, 154704 (2015).
28. S.Y. Bhide, M.L. Berkowitz, J. Chem. Phys. **123**, 224702 (2005).
29. C. Calero, H.E. Stanley, G. Franzese, Materials **9**, 319 (2016).
30. L. Piatkowski, J. de Heij, Huib J. Bakker, J. Phys. Chem. B **117**, 1367 (2013).
31. M.L. Berkowitz, R. Vacha, Acc. Chem. Res. **45**, 74 (2012).
32. M. Stepniewski, A. Bunker, M. Pasenkiewicz-Gierula, M. Karttunen, T. Rog, J. Phys. Chem. B **114**, 11784 (2010).
33. E.A. Disalvo, A. Hollmann, M.F. Martini, Sub-cell. Biochem. **71**, 213 (2015).
34. O.A. Pinto, A.M. Bouchet, M.A. Frias, E.A. Disalvo, J. Phys. Chem. B **118**, 10436 (2014).
35. J. Seelig, P. Ganz, Biochemistry **30**, 9354 (1991).
36. M. Fernandez-Vidal, S.H. White, A.S. Ladokhin, J. Membrane Biol. **239**, 5 (2011).
37. G. Hummer, J.C. Rasaiah, J.P. Noworyta, Nature **414**, 188 (2001).
38. E.P. Schulz, L.M. Alarcón, G.A. Appignanesi, Eur. Phys. J. E **34**, 114 (2011).